

Studying the effect of space radiation induced defects in multijunction solar cell using APSYS simulation software and comparison with the experimental data

Uma BhagyaRajasekaraiah ^{a,*}, Ankush Saini ^a, Sheeja Krishnan ^b, Radhakrishna Vatedka ^a

^a U.R. Rao Satellite Centre, VimanapuraPost, Bengaluru 560017, India

^b ShreeDevi Institute of Technology, Kenjark, Mangalore, India



ARTICLE INFO

Keywords:

Trap concentration
Capture cross section
Finite element analysis
Displacement damage

ABSTRACT

In this paper, the state-of-the-art triple junction solar cell with three sub cells and two tunnel diodes is modeled using two dimensional (2D) APSYS finite element analysis software tool. The effect of electron radiation at 1 MeV and 10 MeV energies for different fluences are investigated by introducing different trap levels, trap states and trap concentrations in InGaP top and InGaAs middle sub cells. Two different structures are modeled by varying layer thickness of base and emitter of both top and middle sub cells to understand its effect on the electrical parameters and efficiency of the solar cell. The main indicative parameters - trap concentration and carrier lifetime is affected by the radiation resulting in alteration of electrical performance of solar cells. The radiation induced defects cause permanent damage to the solar cell structure and degrades the electrical performance of solar cells until its end of life (EOL). In this work, APSYS software tool is used to model radiation induced traps with different trap concentrations, generated the electrical parameters and compared with the experimental results. The results obtained from simulation are in good agreement with the experimental data. Probable traps, trap concentrations and carrier lifetime for different electron radiation energies and fluences were extracted by simulation, which can prove to be difficult to perform experimentally as only a few methods like deep level trap spectroscopy and deep level optical spectroscopy exist for deep level trap studies. This study can therefore save valuable R&D time and cost..

1. Introduction

Photovoltaic solar cells are the main power source for the near earth and interplanetary satellites because of their low cost, robustness, radiation resistance and reliability. The realised efficiency of present-day single junction solar cells made of Si is ~24.7 % and GaAs is 28.2 %, however practical solar cells with 13.5 % (Si) efficiency and 18.5 % (GaAs) are available for space application [1,2]. With improvements in solar cell technology, state-of-the-art multijunction solar cells with conversion efficiency up to 30–32 % are commercially available [1] for space use. Multijunction solar cells (MJSC) are formed or constructed by monolithically connected two or more semiconductor p-n junctions and tunnel diodes to utilize the full sun spectrum to improve the efficiency of solar cells [3] and specific power of the solar panels which is of great value in satellites. Lattice matched GaInP/GaAs/Ge triple junction solar cells with 30–32 % efficiency are extensively used in the space industry

for power generation [1,3].

Multijunction solar cells consists of GaInP top junction with band gap energy of 1.7 eV-1.9 eV, GaAs middle junction with 1.3 eV- 1.4 eV, and a Ge bottom junction with 0.7 eV. In a monolithic solar cell structure, lattice matching of different subcells plays a very important role in improving solar cell efficiency. Middle GaAs and bottom Ge solar cells are lattice mismatched by 0.08 % causing internal thermal stresses in the layers. This mismatch results in dislocations in the GaAs and affects the performance of the solar cell. To overcome this, 1 % indium is added to GaAs, resulting in InGaAs middle solar cell with excellent lattice matching with both Ge bottom cell and InGaP top cell. The resultant multijunction solar cell utilizes the full solar spectrum from nearly 300 nm to 1800 nm and generates more photocurrent with improved efficiency [4,5].

Space radiation consists of energetic protons and electrons [6] of different energies. The main interactions of concern while solar cells are

* Corresponding author.

E-mail address: uma@ursc.gov.in (U. BhagyaRajasekaraiah).

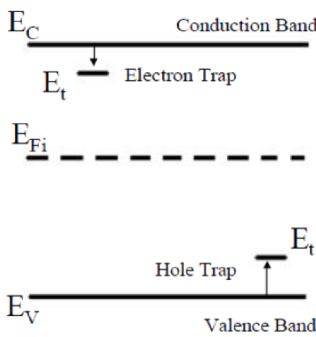


Fig. 1. Hole and electron trap in PN junction.

Table 1
Material properties of InGaP and InGaAs.

Parameter	InGaAs	InGaP
Band gap (eV)	1.405	1.85
Effective mass(m_n)	0.067	0.11
Minority electron lifetime τ_n^0 (s)	2e-8	5e-9
Mobility μ_n ($\text{cm}^2\text{V}^{-1}\text{s}^{-1}$)	3000	400
Diffusion coefficient(cm^2/s)	77.58	10.34
Diffusion length L_n (μm)	12.456	1.017
Thermal velocity V_{th} (cm/s)	4.16×10^7	3.24×10^7

cells are developed [7]. In the development of solar cell technology, finite element analysis/virtual wafer fabrication software like APSYS and SILVACO are extensively [8–11] used as they save valuable R & D time and cost [10]. These simulation models not only have the capability in device optimization but also help to improve the understanding of the effect of material properties and performance characteristics.

APSYS is the state-of-the-art TCAD simulation tool for semiconductor devices and processes. Numerical simulations are carried out by finite element analysis on two-dimensional(2D) 3 J solar cell structures for the solution of Poisson's equation and drift-diffusion current equations with and without radiation induced trap levels in the p-type base layer of the PN junction with active p & n-type layers. Modeling of multijunction solar cells was earlier reported by Sherif Michael et al. [8], Aaron L et al. [9], by using SILVACO virtual wafer fabrication and Z.Q. Li et al. [10], Siva Kotamraju et al. [11] using APSYS.

In this study, APSYS Cross Light software is used for two-dimensional simulation on the triple-junction GaInP/GaAs/Ge solar cell stack. 2D layer development of the device, JV curve plotting, and extraction of electrical parameters are carried out by software simulation. A detailed study is carried out to explore the effect of electron radiation on GaInP/(In)GaAs/Ge solar cells by introducing trap concentration, trap levels in the GaInP top cell, and (In) GaAs middle cells in the model. In all previously reported modeling works, more emphasis has been given to theoretical modeling with no comparison or validation of the simulation results with experimental data. Comparison of the simulated results with

Table 2
List of Doping density in cm^{-3} , layer thickness in μm , and mole fraction of different layers and type of materials.

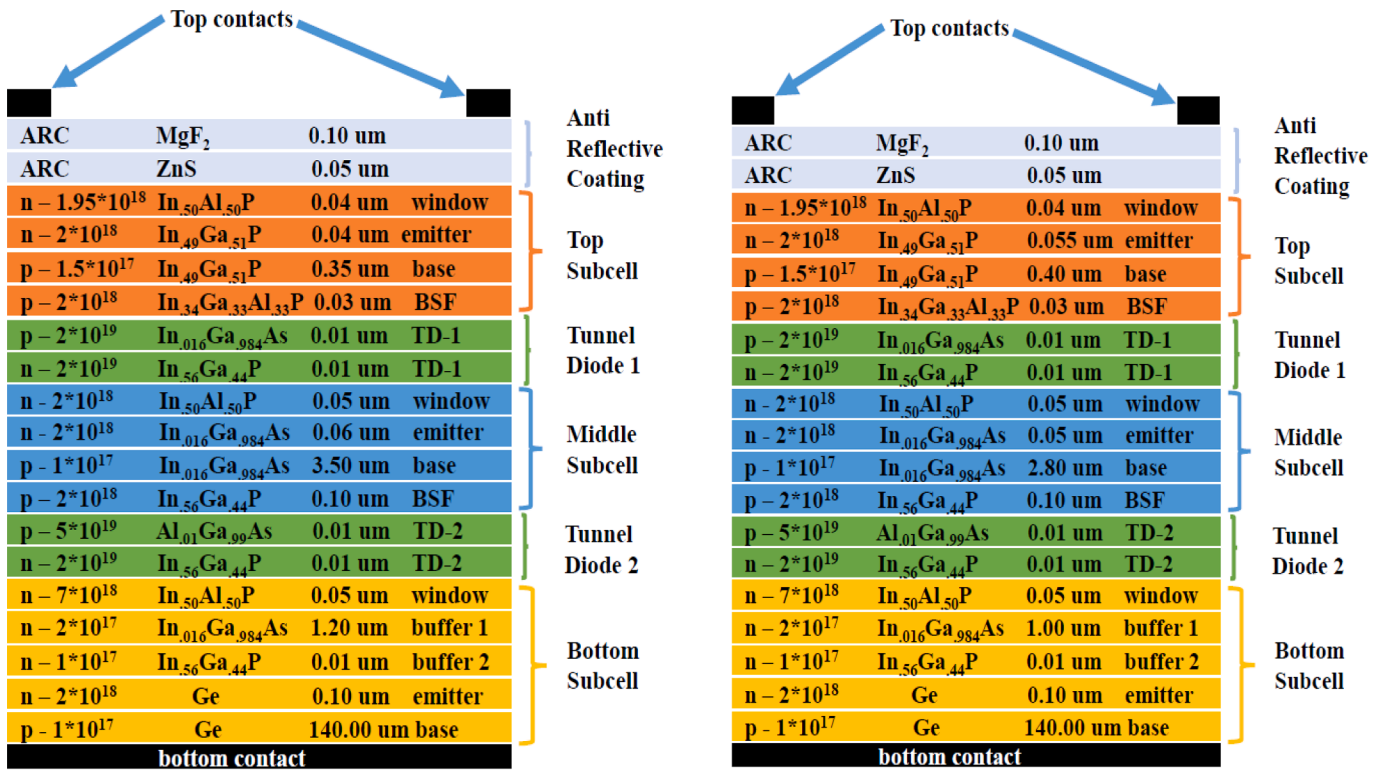
Layer No.	Material	Anticipated Thickness (μm)	Doping concentration (cm^{-3})	Bandgap/Energy gap in eV	Remarks
19	MgF ₂	0.01			ARC
18	ZnS	0.05			ARC
17	n ⁺ -In _{0.50} Al _{0.50} P	0.04	1.95×10^{18}	2.455	Window
16	n ⁺ -In _{0.49} Ga _{0.51} P	0.04	2×10^{18}	1.757	Emitter
15	p ⁺ -In _{0.49} Ga _{0.51} P	0.35	1.5×10^{17}	1.757	Base
14	p ⁺ -In _{0.34} Ga _{0.33} Al _{0.33} P	0.03	2×10^{18}	2.446	Back surface field (BSF)
13	p ⁺⁺ -In _{0.016} Ga _{0.984} As	0.010	2×10^{19}	1.426	Tunnel Diode
12	n ⁺⁺ -In _{0.56} Ga _{0.44} P	0.010	2×10^{19}	1.681	
11	n ⁺ -In _{0.50} Al _{0.50} P	0.05	2×10^{18}	2.455	
10	n ⁺ -In _{0.016} Ga _{0.984} As	0.06	2×10^{18}	1.426	Window layer
9	P ⁺ -In _{0.016} Ga _{0.984} As	3.5	1×10^{17}	1.426	Emitter
8	p ⁺ -In _{0.56} Ga _{0.44} P	0.1	2×10^{18}	1.681	Base
7	p ⁺⁺ -Al _{0.01} Ga _{0.99} As	0.01	5×10^{19}	1.436	Back surface field
6	n ⁺⁺ -In _{0.56} Ga _{0.44} P	0.01	2×10^{19}	1.681	Tunnel Diode
5	n ⁺ -In _{0.50} Al _{0.50} P	0.05	7×10^{18}	2.455	
4	n ⁺ -In _{0.016} Ga _{0.984} As	1.2	2×10^{17}	1.426	Buffer 2
3	n ⁺ -In _{0.56} Ga _{0.44} P	0.01	1×10^{17}	1.681	Buffer 1
2	n ⁺ -Ge	0.1	2×10^{18}	0.67	Emitter
1	p ⁺ -Ge	140	1×10^{17}	0.67	Substrate(base)

irradiated with electron and proton radiation are ionization and atomic displacement [6]. Atomic displacement occurs when energetic particles interact with the atomic structure and result in the displacement of atoms within the material's structure. A displaced atom within the crystal lattice will result in the formation of an interstitial defect atom, a vacancy, and other electronic and phonon losses. Displaced atoms will form stable defects (Fig.1) and cause permanent degradation in the solar cell performance [6–9]. As a result, these defects acts as acceptor or donor like energy states within the energy gap of the material. The introduction of these type of traps/ defects reduces the minority carrier life and affects the performance.

To meet the increased demand in the power requirement of satellites, high efficiency lattice matched three, four, and up to five junction solar

experimental data is very important and it helps to validate the modeled solar cell structure and radiation effect. Novelty of this study is that more emphasis is given to simulate the radiation damage on solar cells by introducing different trap concentration which is equivalent to the accumulated fluence experienced by solar cells in space in its mission life.

For the experimental study the space grade solar cells which are used in many spacecrafts are used. The current density–voltage (J-V) characteristics are generated by simulation and compared with the measured JV data at one Air mass zero (1 AM0) spectrum. From the simulation, the effect of radiation on short circuit current density (J_{sc}), open circuit voltage (V_{oc}), and efficiency (η) are studied for different energy and fluences by introducing different traps in both top and middle cells. In



(a)Structure 1with 29% efficiency

(b) Structure 2with 28.5% efficiency

Fig. 2. Triple junction (3 J) structure with different mole fraction, junction thickness, and doping concentration (cm^{-3}) (a) is for 29 % efficiency and (b) for 28.5 % efficiency.

Table 3
The layer thickness of different layers corresponds to two structures.

Layer	29 % efficient structure(1)	28.5 % efficient structure(2)
	Thickness (μm)	Thickness (μm)
Top cell	Emitter 0.04	0.055
	Base 0.35	0.4
Middle cell	Emitter 0.06	0.05
	Base 3.5	2.8
	Buffer 1.2	1
	1	

this study, different material combinations and mole fractions are also explored to improve the bandgap and lattice matching of the solar cell structure. The electrical parameters obtained from the simulation are compared with the experimental results. The study of defects in solar cell is very critical as only few experimental methods like deep level trap spectroscopy and deep level optical spectroscopy exist for deep level trap studies. DLTS characterisation method is time consuming and requires special expertise for sample preparation and it is even more difficult for multijunction solar cell compared to single junction cell as MJSC have many junctions. Hence in multijunction solar cell radiation studies, simulation software plays very important role.

2. Modeling and simulation of Multi-junction solar cell structure

The multijunction solar cell is modeled using 2D Cross light simulation software. The solar cell contains three PN junctions, window layer, tunnels diodes, buffer layer and BSF layers, these layers are built by using layer builder option in the software. The material selection, material properties were taken from material library. The multijunction

solar cell is modeled by using the basic material properties of the InGaP top cell and InGaAs middle cell are listed in [Table 1](#). The material combinations of different layers, doping density (cm^{-3}), layer thickness (in μm), and mole fraction of different layers are taken from literature [\[10–12\]](#) and the details are listed in [Table 2](#). The sub cells thickness are optimized to improve the absorption of incident photons which improves the efficiency of solar cell. The thinner the solar cell, the transmission of photons will be more. In triple junction, cell thinning of the top cell will allow photons to pass through the top cell and reach the other sub cells reappportioning the light between the sub cells resulting in good current matching. Hence in multijunction cells, the cell efficiency will be maximized when the top sub cell is thinned for better current matching. After many iterations the solar cell structure is finalized, each time JV curve was generated and compared with the JV curve of practical solar cell. Two MJSC structures are finalized for this work based on the electrical parameters which are more comparable with the electrical parameter of practical solar cell.

The effect of radiation is modeled on triple-junction full cells by introducing traps in both top and middle junction cells with different capture cross sections and trap concentrations [\[11–14\]](#). The list of trap level, type of trap, corresponding capture cross section, and trap concentration [\[14–18\]](#) for 10 MeV and 1 MeV electron radiation are listed in [Tables 4 and 5](#). The range of values is selected based on different reference papers [\[14–18\]](#). Many iterations were tried with different trap parameters and different simulation runs by keeping the material properties and solar cell structure same. The JV characteristics were generated from the simulation and compared with the experimental values, the values which are in good comparison with experimental data are chosen, and the carrier lifetime is calculated for the selected parameters.

In this study, two triple junction solar cell structures with different

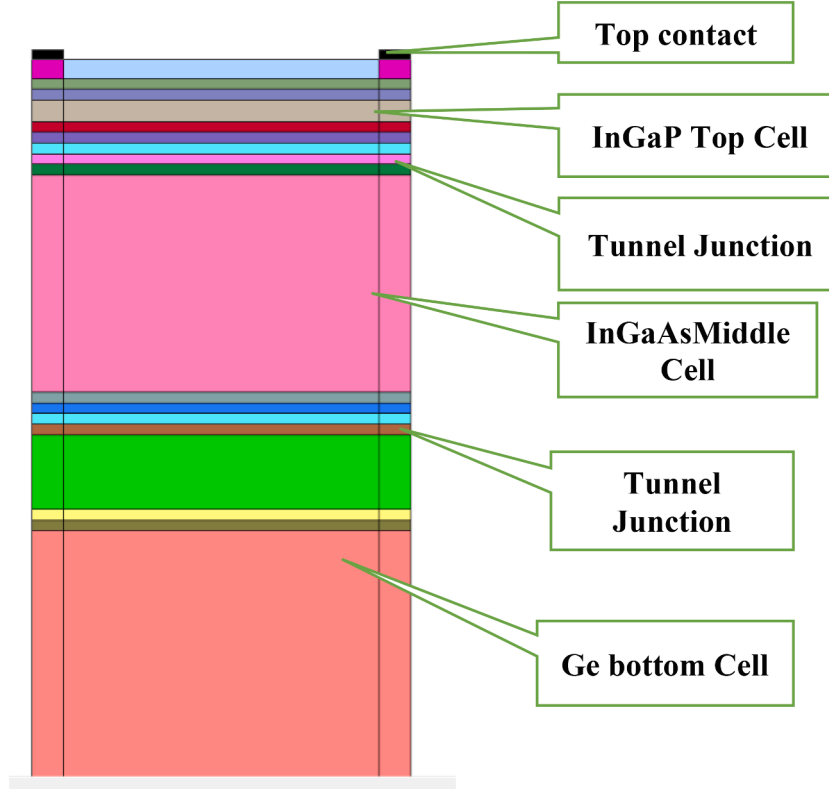


Fig. 3. Screenshot of layer builder of APSYS (not to scale).

layers are built by using layer builder in the APSYS. By varying the thickness of base and emitter layers of both top cell and middle cell structures, two cells with different efficiencies were developed. The modeled structures are shown in Fig. 2, named as structure 1 for 29 % efficiency and structure 2 for 28.5 % efficiency. The purpose of developing two different structures is to understand the effect of different layer thickness on the electrical output and efficiency of the solar cell.

The efficiency of solar cell is $\eta = \frac{P_{max}}{P_{in}}$

$$\eta = \frac{V_{oc}I_{sc}FF}{P_{in}} \quad (1)$$

The difference in the layer thicknesses of the two structures is listed in Table 3. From the table, it can be seen that the base and emitter thickness will affect the overall performance and efficiency of the solar cell. An increase in the layer thickness in the top cell will reduce photon absorption and results in lower efficiency. The screenshot of the layer builder is shown in Fig. 3.

The radiation induced defects are introduced in both valence band edge (E_v) and conduction band edge (E_c) with different traps in InGaP middle cell at $E_v - 0.9$ and in InGaP top cell at $E_v - 0.36$, $E_v - 0.72$, $E_c + 0.5$, $E_c + 0.76$, with varying trap capture cross section and trap concentration (N_t). The capture cross section and trap concentration values are taken from different reference papers [11–13].

The approximate values of the capture cross section used in the model corresponding to the trap levels are listed in Tables 4 and 5 for structures 1 and 2 respectively [19–23]. The minority carrier lifetime plays an important role in the performance of the solar cell and is estimated for both top p-InGaP, middle p-InGaAs cells.

The effective lifetime τ_n is given as:

$$\frac{1}{\tau_n} = \frac{1}{\tau_n^0} + \frac{1}{\tau_{rad}} + \frac{1}{\tau_{nonrad}} \quad (2)$$

Where,

τ_n^0 is minority electron lifetime without traps, τ_{rad} is the lifetime of radiative recombination and τ_{nonrad} is the lifetime due to non-radiative recombination.

Since lifetime of radiative recombination τ_{rad} for a multijunction solar cell is negligible [11], hence the carrier lifetime after radiation is τ_{nonrad} is given as:

$$\tau_{nonrad} = \frac{1}{N_t \sigma V_{th}} \quad (3)$$

Where, N_t is trap concentration, σ is capture cross section and V_{th} is thermal velocity a constant for material at the given temperature and can be expressed as:

$$V_{th} = \sqrt{\frac{8kT}{m_n}} \quad (4)$$

Where, k is the Boltzmann's constant, T is the temperature and m_n is the effective mass and the value is listed in Table 1.

The relation between trap concentration and radiation fluence is given by (11, 20)

$$N_t = k\phi \quad (5)$$

Where N_t is trap concentration, ϕ is radiation fluence. k is the introduction rate of non radiative centers, it is not the only factor but various

Table 4

Electron and Hole trap levels, capture cross section, and trap concentration for 10 MeV and 1 MeV electron radiation at different fluences for structure 1.

Fluence e/ cm ²	Material Type	Trap level	Capture Cross section σ (cm ⁻²)	Type	10 MeV electron energy		1 MeV electron energy	
					Lifetime in sec	Trap Concentration $N_t(\text{cm}^{-3})$	Lifetime in sec	Trap Concentration $N_t(\text{cm}^{-3})$
1.00E + 14	InGaAs	Ec-0.9	2.00×10^{-12}	Acceptor	4.81×10^{-09}	2.50×10^{12}	5.23×10^{-09}	2.30×10^{12}
	InGaP	Ec-0.36	3.00×10^{-17}	Acceptor	1.34×10^{-09}	6.00×10^{17}	1.34×10^{-09}	6.00×10^{17}
	InGaP	Ec-0.72	2.50×10^{-17}	Acceptor	1.37×10^{-09}	7.00×10^{17}	1.37×10^{-09}	7.00×10^{17}
	InGaP	Ev + 0.5	4.00×10^{-16}	Donor	2.57×10^{-09}	3.00×10^{16}	2.57×10^{-09}	3.00×10^{16}
	InGaP	Ev + 0.76	5.00×10^{-16}	Donor	3.08×10^{-09}	2.50×10^{16}	2.47×10^{-09}	2.00×10^{16}
	InGaAs	Ec-0.9	2.00×10^{-12}	Acceptor	6.68×10^{-10}	1.80×10^{13}	1.85×10^{-09}	6.50×10^{12}
5.00E + 14	InGaP	Ec-0.36	3.00×10^{-17}	Acceptor	1.00×10^{-09}	8.00×10^{17}	1.14×10^{-09}	8.00×10^{17}
	InGaP	Ec-0.72	2.50×10^{-17}	Acceptor	1.072×10^{-09}	9.00×10^{17}	1.2×10^{-09}	8.00×10^{17}
	InGaP	Ev + 0.5	4.00×10^{-16}	Donor	9.63×10^{-10}	8.00×10^{16}	1.10×10^{-09}	7.00×10^{16}
	InGaP	Ev + 0.76	5.00×10^{-16}	Donor	8.81×10^{-10}	7.00×10^{16}	1.12×10^{-09}	5.50×10^{16}
	InGaAs	Ec-0.9	2.00×10^{-12}	Acceptor	1.72×10^{-10}	7.00×10^{13}	8.59×10^{-10}	1.40×10^{13}
	InGaP	Ec-0.36	3.00×10^{-17}	Acceptor	2.00×10^{-10}	4.00×10^{18}	5.34×10^{-10}	1.50×10^{18}
1.00E + 15	InGaP	Ec-0.72	2.50×10^{-17}	Acceptor	1.20×10^{-10}	8.00×10^{18}	4.81×10^{-10}	2.00×10^{18}
	InGaP	Ev + 0.5	4.00×10^{-16}	Donor	8.56×10^{-10}	9.00×10^{16}	1.04×10^{-09}	7.40×10^{16}
	InGaP	Ev + 0.76	5.00×10^{-16}	Donor	7.71×10^{-10}	8.00×10^{16}	9.94×10^{-10}	6.20×10^{16}
	InGaAs	Ec-0.9	2.00×10^{-12}	Acceptor	2.67×10^{-11}	4.50×10^{14}	4.01×10^{-10}	3.00×10^{13}
	InGaP	Ec-0.36	3.00×10^{-17}	Acceptor	1.00×10^{-10}	8.00×10^{18}	2.67×10^{-10}	3.00×10^{18}
	InGaP	Ec-0.72	2.50×10^{-17}	Acceptor	1.07×10^{-10}	9.00×10^{18}	3.00×10^{-10}	3.20×10^{18}
3.00E + 15	InGaP	Ev + 0.5	4.00×10^{-16}	Donor	3.85×10^{-10}	2.00×10^{18}	9.63×10^{-10}	8.00×10^{16}
	InGaAs	Ec-0.9	2.00×10^{-12}	Acceptor	5.00×10^{-16}	1.00×10^{16}	9.48×10^{-10}	6.50×10^{16}
	InGaP	Ec-0.36	3.00×10^{-17}	Acceptor	1.00×10^{-10}	8.00×10^{18}	2.67×10^{-10}	3.00×10^{18}
	InGaP	Ec-0.72	2.50×10^{-17}	Acceptor	1.07×10^{-10}	9.00×10^{18}	3.00×10^{-10}	3.20×10^{18}
	InGaP	Ev + 0.5	4.00×10^{-16}	Donor	3.85×10^{-10}	2.00×10^{17}	9.63×10^{-10}	8.00×10^{16}
	InGaP	Ev + 0.76	5.00×10^{-16}	Donor	6.17×10^{-10}	1.00×10^{17}	9.48×10^{-10}	6.50×10^{16}

Table 5

Electron and Hole trap levels, capture cross section, and trap concentration for 1 MeV electron radiation at different fluences for structure 2.

Electron radiation fluence e/cm ²	Material Type	Trap level	Capture Cross section σ (cm ⁻²)	Carrier Type	Life time in sec	Trap Concentration $N_t(\text{cm}^{-3})$
1.00E + 13	InGaAs	Ec-0.9	2.00×10^{-12}	acceptor	1.34×10^{-08}	9.00×10^{11}
	InGaP	Ec-0.36	3.00×10^{-17}	acceptor	8.90×10^{-09}	9.00×10^{16}
	InGaP	Ec-0.72	2.50×10^{-17}	acceptor	9.62×10^{-09}	1.00×10^{17}
	InGaP	Ev + 0.5	4.00×10^{-16}	donor	3.85×10^{-09}	2.00×10^{16}
	InGaP	Ev + 0.76	5.00×10^{-16}	donor	6.17×10^{-09}	1.00×10^{16}
	InGaAs	Ec-0.9	2.00×10^{-12}	acceptor	5.23×10^{-09}	2.30×10^{12}
1.00E + 14	InGaP	Ec-0.36	3.00×10^{-17}	acceptor	1.34×10^{-09}	6.00×10^{17}
	InGaP	Ec-0.72	2.50×10^{-17}	acceptor	1.37×10^{-09}	7.00×10^{17}
	InGaP	Ev + 0.5	4.00×10^{-16}	donor	2.57×10^{-09}	3.00×10^{16}
	InGaP	Ev + 0.76	5.00×10^{-16}	donor	2.47×10^{-09}	2.50×10^{16}
	InGaAs	Ec-0.9	2.00×10^{-12}	acceptor	1.85×10^{-09}	6.50×10^{12}
	InGaP	Ec-0.36	3.00×10^{-17}	acceptor	1.00×10^{-09}	8.00×10^{17}
5.00E + 14	InGaP	Ec-0.72	2.50×10^{-17}	acceptor	1.07×10^{-09}	9.00×10^{17}
	InGaP	Ev + 0.5	4.00×10^{-16}	donor	1.10×10^{-09}	7.00×10^{16}
	InGaP	Ev + 0.76	5.00×10^{-16}	donor	1.12×10^{-09}	5.50×10^{16}
	InGaAs	Ec-0.9	2.00×10^{-12}	acceptor	1.85×10^{-09}	6.50×10^{12}
	InGaP	Ec-0.36	3.00×10^{-17}	acceptor	1.00×10^{-09}	8.00×10^{17}
	InGaP	Ec-0.72	2.50×10^{-17}	acceptor	1.07×10^{-09}	9.00×10^{17}
1.00E + 15	InGaP	Ev + 0.5	4.00×10^{-16}	donor	1.10×10^{-09}	7.00×10^{16}
	InGaAs	Ec-0.9	2.00×10^{-12}	acceptor	8.59×10^{-10}	1.40×10^{13}
	InGaP	Ec-0.36	3.00×10^{-17}	acceptor	5.34×10^{-10}	1.50×10^{18}
	InGaP	Ec-0.72	2.50×10^{-17}	acceptor	4.81×10^{-10}	2.00×10^{18}
	InGaP	Ev + 0.5	4.00×10^{-16}	donor	1.04×10^{-09}	7.40×10^{16}
	InGaP	Ev + 0.76	5.00×10^{-16}	donor	9.94×10^{-10}	6.20×10^{16}

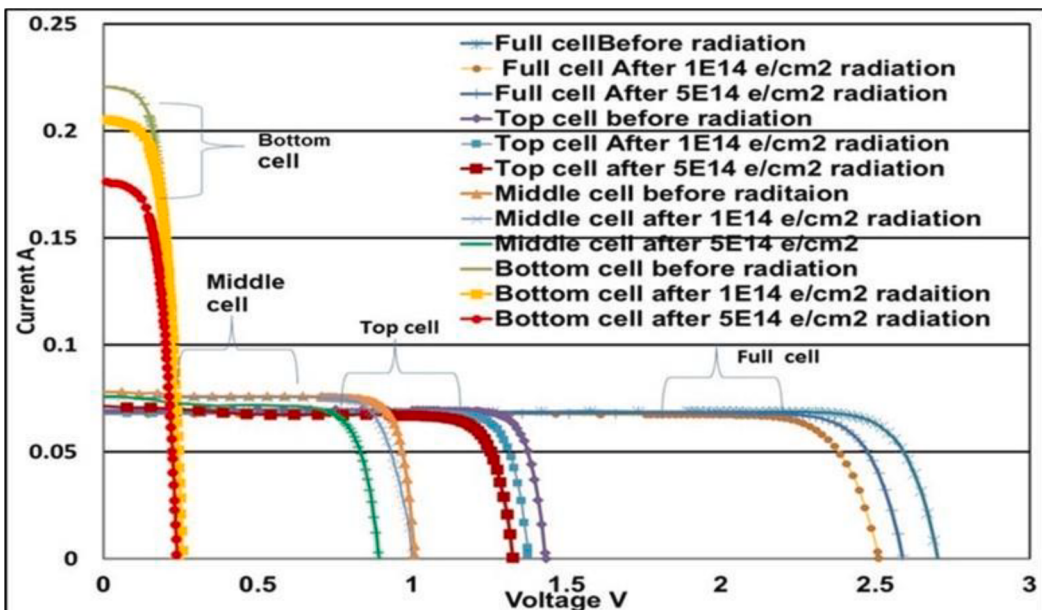


Fig. 4. Pre and post radiation Current-Voltage (IV) characteristics of sub cells and full cell for 1 MeV.

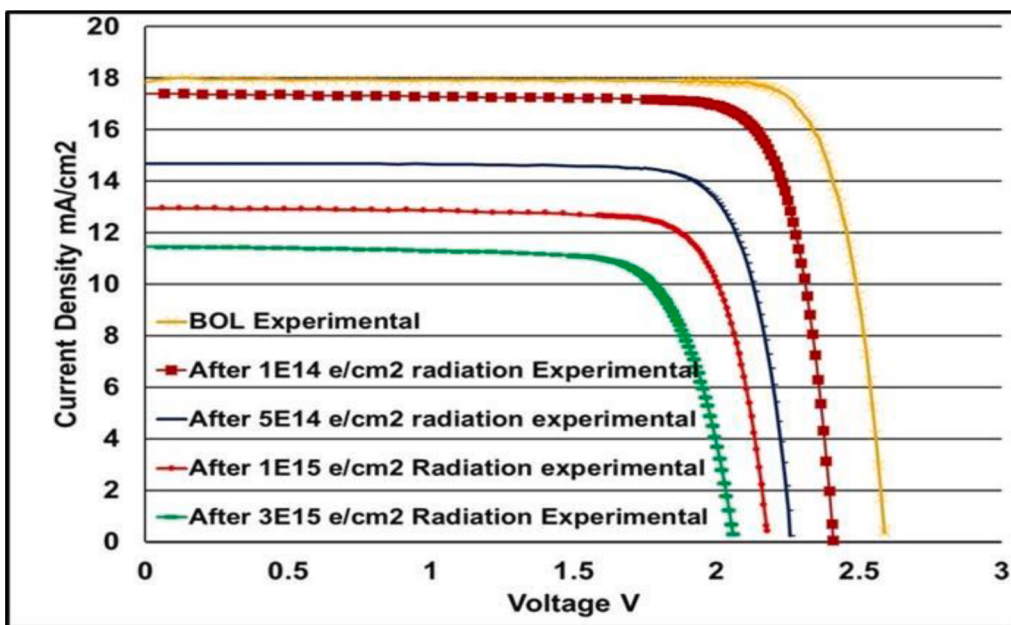


Fig. 5. Current density (J)- Voltage characteristics of structure 1 for 10 MeV electron radiation – Experiment results.

defects are created by radiation and only fraction of these behaves as recombination centers. The introduction rate depends on material and energy/fluence of the particle.

3. Experimental details

The space grade multijunction solar cells from two different manufacturers which are flown in many spacecrafts are considered for this study. The solar cells are modeled with different material combinations and mole fractions and named as structure 1 and structure 2. The JV characteristics are generated and compared with the JV of space grade multijunction solar cells. The modelled solar cell JV is compared with the JV of space grade solar cell and matched cell is interpreted as structure 1 and 2. The space grade solar cells were irradiated with 1 MeV electron radiation at room temperature by using DC accelerator and are

irradiated with 10 MeV electron radiation using RF LiNAC (Linear Particle Accelerator) at Electron Beam Center (EBC), Bhabha Atomic Research Center (BARC), Mumbai. The electron radiation is considered in this study because in space solar cell/spaceship radiation study, all the energies of proton and electron are converted in to 1 MeV electron and equivalence is calculated.

The solar cell current-voltage characterization is carried out for 1 AM0 spectrum by using X-25 sun simulator at 28C at Solar Panels Division, U.R. Rao Satellite center (URSC). X-25 solar simulator is calibrated using secondary standard set generated by balloon flight standards. The solar cells were characterized pre and post radiation under the same condition at 28C.

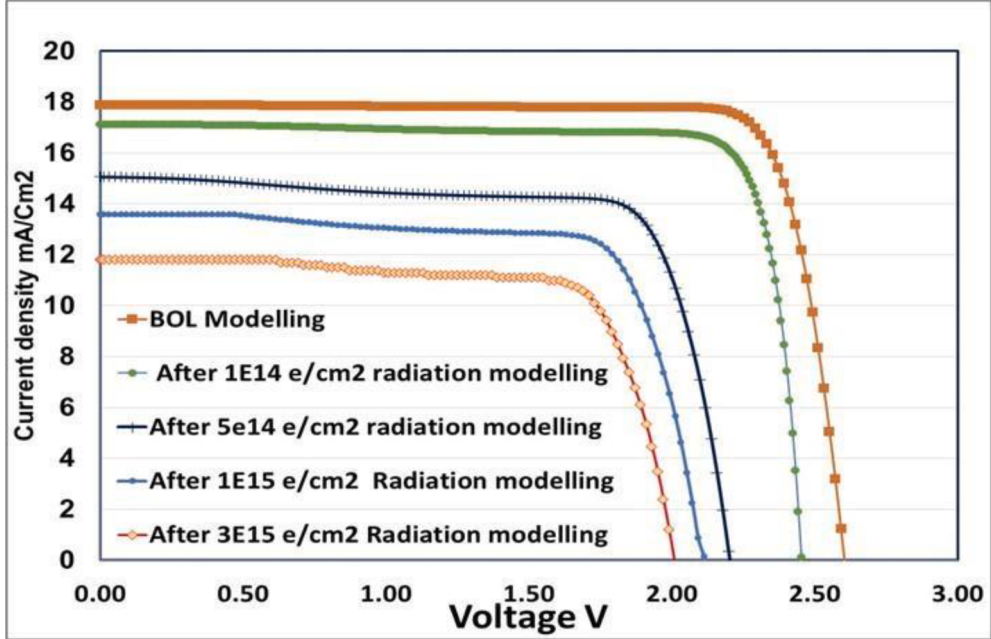


Fig. 6. Current density (J)- Voltage characteristics of structure1 for 10 MeV electron radiation –simulation results.

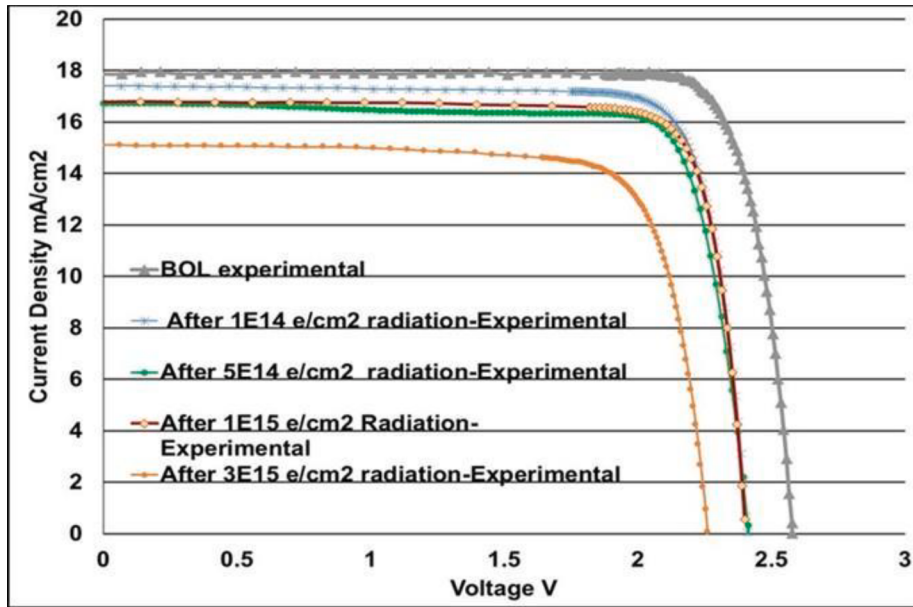


Fig. 7. Current density (J)- Voltage characteristics of structure 1 for 1 MeV electron radiation –Experiment results.

4. Results and analysis

Multijunction solar cell used in this simulation is made of lattice matched three sub cells, the sub cells of multijunction solar cells respond to different wavelengths and generate current and voltages. The top cell generates 17.5 mA/cm² short circuit current density (J_{sc}), 1.45V voltage (V_{oc}), the middle cell generates 18.5 mA/cm² current, 1.1 V voltage, and the low bandgap Ge bottom cell generates higher current density 50 mA/cm² current, lower voltage 0.250 V. Since the multijunction solar cell is a monolithically series connected structure, the lower current generated by the top cell limits the full cell current and the voltage of all sub cells is added. The typical current of the full cell is 17.5 mA/cm² and the generated voltage is added and open circuit voltage is 2.6 V. The pre and post radiation IV characteristics of all sub cells and full cells are

shown in Fig. 4 which represents how the electrical parameter of each subcell will change after radiation exposure for 1 MeV electron energy. IV plot of 10 MeV is similar to 1 MeV with more degradation in the electrical parameters, as higher energy particles create more recombination centers and degrades more [24].

The Systematic study on the effect of radiation is carried out on MJSC structure 1 for both 10 MeV and 1 MeV electron radiation at 1E14, 5E14, 1E15 and 3E15 e/cm² fluences by introducing different traps. The simulated JV is compared with JV of practical solar cell for each fulence. Several traps levels will be created by energetic radiation which are present in space environment, however it was experimentally proven that (A. Khan et al. [13,18]) E_c = -0.36, E_c = -0.72, E_v = +0.5 and E_v = +0.76 are the main non-radiative recombination centres for InGaP top cell and for InGaAs middle layer E_c = -0.9 is the main trap centre

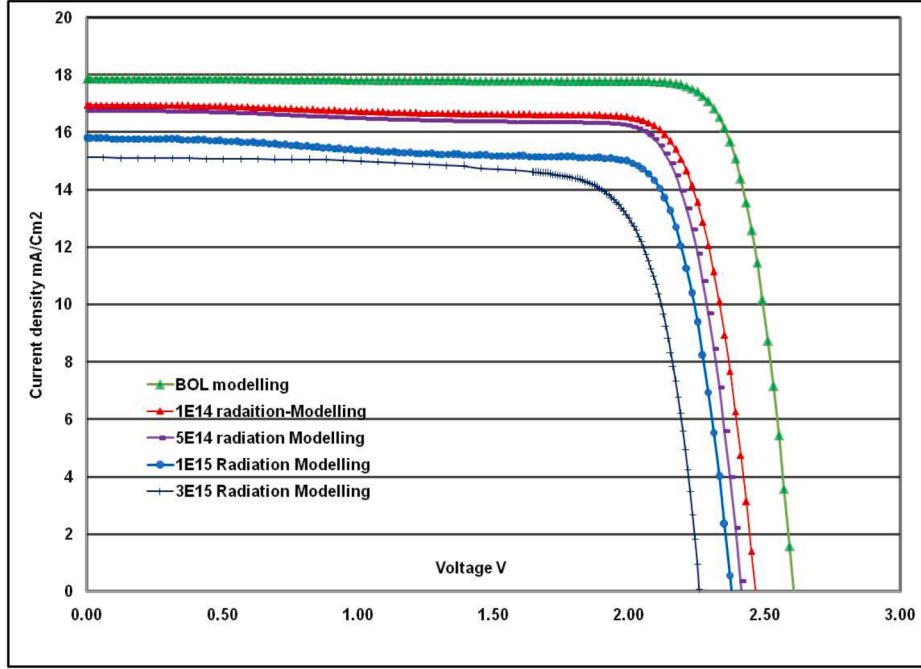


Fig. 8. Current density (J)- Voltage characteristics of structure 1 for 1 MeV electron radiation -Simulation results.

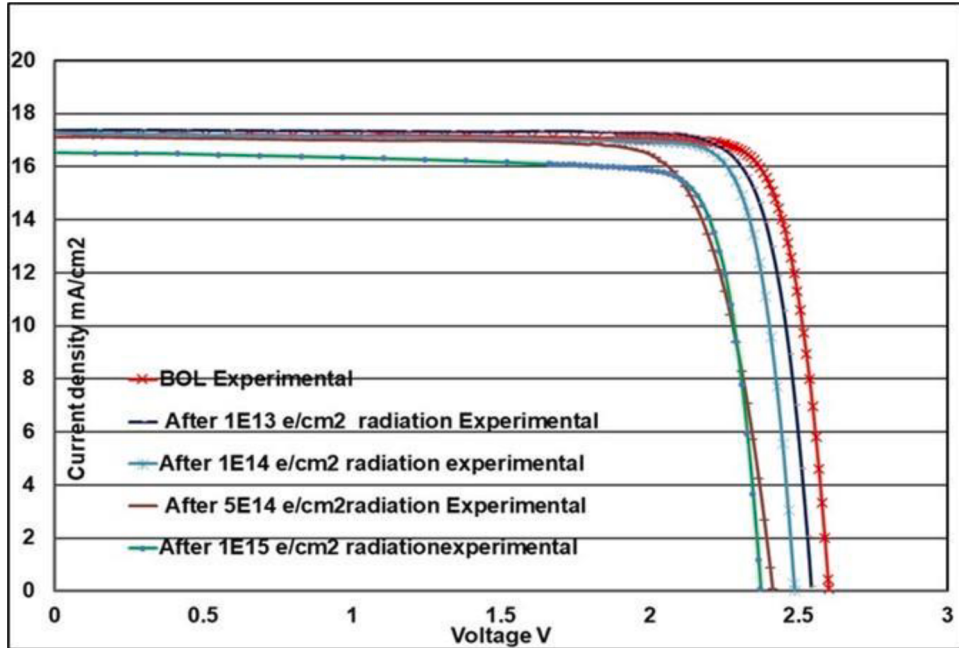


Fig. 9. Current density (j)- voltage characteristics of structure 2 for 1 MeV electron radiation -Experiment results.

(Danilchenko et al.), hence for this study these trap centers were considered and used for simulation and modeling for all fluencies.

For each fluence, current density (J) – voltage (V) characteristics are generated from the simulation and compared with the experimental J-V characteristics. The experimental J-V characteristic for 10 MeV electron energy of structure 1 at different fluencies is shown in Fig. 5. The simulated JV characteristic at different fluencies is shown in Fig. 6. Similarly, for 1 MeV electron energy, the experimental data at different fluencies is shown in Fig. 7 and simulated JV data is shown in Fig. 8.

Similarly MJSC structure 2 is studied for 1 MeV electron radiation for 1E13 e/cm², 1E14 e/cm², 5E14 e/cm² and 1E15 e/cm² fluences. The details of trap levels capture cross section, and trap concentrations are

listed in Table 5. The J-V characteristics of experimental and simulation are shown in Figures 9 and 10.

The comparison of results indicates that the J_{sc} , V_{oc} and efficiency (η) of simulation are in good match with the experimental data. The difference is about < 4 %, the data is listed in Tables 6 and 7, similar deviation is reported by Sherif Michel et al. [8] with SILVACO virtual wafer fabrication. From this study, the trap parameters were extracted from simulation for different electron radiation energies and fluencies, which is otherwise difficult experimentally.

As given in Tables 6 and 7 for 1 MeV electron radiation the efficiency of structure 1 cell degrades 6.03 % from 28.58 (BOL) to 22.55 (1.00E + 15 e/cm²) while the efficiency of structure 2 cell degrades only 4.25 %

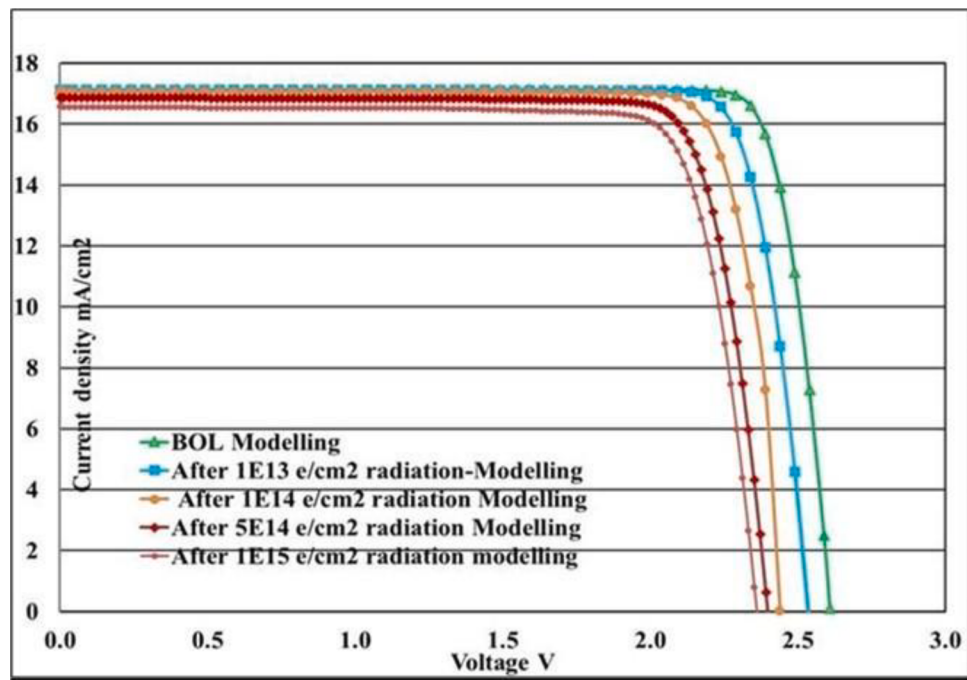


Fig. 10. Current density (J)- Voltage characteristics of structure2 for 1 MeV electron radiation -simulation results.

Table 6

Comparison of simulation data and experiment data for structure 1 cell for 10 MeV and 1 MeV electron energy.

Electron radiation fluence e/cm ²	Parameters	10 MeV energy			1 MeV energy		
		Simulation results	Experiment results	Deviation (%)	Simulation results	Experiment results	Deviation (%)
BOL	Jsc (mA/cm ²)	17.87	17.85	0.112	17.875	17.875	0.000
	Voc(V)	2.59	2.589	0.039	2.61	2.577	1.264
	Efficiency (%)	28.86	28.51	1.213	28.95	28.58	1.278
1E + 14	Jsc (mA/cm ²)	17.67	17.67	0.000	16.96	17.4	2.594
	Voc(V)	2.43	2.429	0.041	2.45	2.409	1.673
	Efficiency (%)	25.03	25.46	1.718	25.13	25.47	1.353
5E + 14	Jsc (mA/cm ²)	15.1	15.07	0.199	16.8	16.9	0.595
	Voc(V)	2.259	2.22	1.726	2.41	2.41	0.000
	Efficiency (%)	18.88	19.5	3.284	24.38	25	2.543
1E15	Jsc (mA/cm ²)	13.4	12.95	3.358	16.35	16.25	0.611
	Voc(V)	2.117	2.17	2.504	2.37	2.33	1.68
	Efficiency (%)	16	16.61	3.813	21.94	22.55	2.488
3E15	Jsc (mA/cm ²)	11.45	11.48	0.262	15.16	15.12	0.264
	Voc(V)	2.05	2.01	1.951	2.35	2.26	3.830
	Efficiency (%)	13.39	13.24	1.120	21.06	20.24	3.894

from 28.37 (BOL) to 24.12 (1.00E + 15 e/cm²), also current density and voltages decreases less for structure 2 compare to stucture1. From the results it is clear that structure 2 shows more radiation hardness than structure 1 and it is attribute to the thickness of the top cell of the structures. This behavior is shown in the simulated results also. The thickness of top cell (base + emitter) in structure 2 is 65 nm more than the thickness of the top cell (base + emitter) of structure 1. Thicker layer of top cell helps in preventing the penetration of electron radiation into the middle cell and reduce the degradation of MJSC.

From Table 6 it is observed that for 10 MeV electron energy the efficiency degrades about 44.55 % from 28.86 %(BOL) to 16 %(1E15e/cm²) it shows that higher energy radiation creates more traps and degradation.

Probable trap levels and trap concentrations were also determined for both 1 MeV and 10 MeV electron radiations at different fluences. In Top InGaP the radiation introduces lower trap concentration in the shallow level and more traps in the deeper level compared to middle GaAs, where as in middle (In) GaAs the radiation introduces less traps

and it creates more damage to the solar cell, the JV curve is plotted for combined traps and the results are listed in Tables 9 and 10. GaAs is more susceptible to radiation compared to InGaP, this is because in case of GaAs-based materials, a higher current density injection or higher temperature annealing is required to anneal out the defects. As the fraction of In and P bonds increases, the introduction rate of the defects decreases, which decreases radiation-induced defects in the material, which is due to simultaneous annealing. The energy required to anneal out defects is less in InGaP-based materials compared to other compound semiconductor materials. The high-radiation-resistant properties of InGaP-related materials are attributed to room temperature annealing of radiation-induced defects [25].

The relation between trap concentration and fluence is given by the equation $N_t = k\phi$, the fitting is carried out by using MATLAB polynomial (degree one) to obtain the defect introduction rate / damage constant for different trap concentration in both middle InGaAs and top InGaP cell. Sample curve fitting for InGaAs ($E_c = -0.9$) is shown in Fig. 11, similar method is followed for all other traps and k value is

Table 7

Comparison of simulation data and experiment data for structure 2 cell for 1 MeV.

Electron radiation fluence e/cm^2		Simulation results	Experimen Results	Deviation (%)
BOL	Jsc (mA/ cm^2)	17.14	17.25	0.64
	Voc(V)	2.64	2.602	0.8
	Efficiency (%)	28.71	28.37	1.3
1.00E + 13	Jsc (mA/ cm^2)	17.1	17.4	2.33
	Voc(V)	2.49	2.512	0.88
	Efficiency (%)	26.99	27.5	2.14
1.00E + 14	Jsc (mA/ cm^2)	17.06	17.3	1.407
	Voc(V)	2.46	2.48	0.813
	Efficiency (%)	26.24	27	2.896
5.00E + 14	Jsc (mA/ cm^2)	16.85	17.02	1.009
	Voc(V)	2.41	2.41	0.000
	Efficiency (%)	24.89	24.42	1.888
1.00E + 15	Jsc (mA/ Cm^2)	16.55	16.51	0.242
	Voc(V)	2.37	2.373	0.127
	Efficiency (%)	23.85	24.12	1.132

Table 8

Extracted defect introduction rate k for different trap levels.

Material type and trap level	1 MeV	10 MeV
InGaAs(middle cell) Ec = -0.9	$k = 1.210(R^2 = 0.982)$	$k = 2.224(R^2 = 0.9699)$
InGaP(Top cell) Ev = +0.5	$k = 2.219(R^2 = 0.9043)$	$k = 7.079(R^2 = 0.973)$
InGaP(Top cell) Ev = +0.76	$k = 5.148(R^2 = 0.972)$	$k = 8.219(R^2 = 0.962)$
InGaP(Top cell) Ec = -0.36	$k = 1.065(R^2 = 0.968)$	$k = 3.290(R^2 = 0.912)$
InGaP(Top cell) Ec = -0.72	$k = 3.289(R^2 = 0.914)$	$k = 6.390(R^2 = 0.952)$

Table 9

The details of trap level, lifetime, trap concentration and JV parameters for 10 MeV electron radiation at both top and middle cell.

Electron radiation fluence e/cm^2	Material Type	Trap level	Lifetime in sec	Trap Concentration $N_t(cm^{-3})$	Jsc (mA/ cm^2)	Voc(V)	η (%)
BOL 1.00E + 14	InGaAs	Ec-0.9	4.81×10^{-9}	2.50×10^{12}	17.87 17.67	2.59	28.86
	InGaP	Ec-0.36	1.34×10^{-9}	6.00×10^{17}		2.43	25.03
	InGaP	Ec-0.72	1.37×10^{-9}	7.00×10^{17}			
	InGaP	Ev + 0.5	2.57×10^{-9}	3.00×10^{16}	15.1		
	InGaP	Ev + 0.76	3.08×10^{-9}	2.50×10^{16}			
	InGaAs	Ec-0.9	6.68×10^{-10}	1.80×10^{13}			
5.00E + 14	InGaP	Ec-0.36	1.00×10^{-9}	8.00×10^{17}	13.4	2.259	18.88
	InGaP	Ec-0.72	1.20×10^{-9}	8.0×10^{17}			
	InGaP	Ev + 0.5	9.63×10^{-10}	8.0×10^{16}			
	InGaP	Ev + 0.76	8.81×10^{-10}	7.00×10^{16}	11.45	2.117	16
	InGaAs	Ec-0.9	1.72×10^{-10}	7.00×10^{13}			
	InGaP	Ec-0.36	2.00×10^{-10}	4.00×10^{18}			
1.00E + 15	InGaP	Ec-0.72	1.20×10^{-10}	8.00×10^{18}	13.4		
	InGaP	Ev + 0.5	8.56×10^{-10}	9.00×10^{16}			
	InGaP	Ev + 0.76	7.71×10^{-10}	8.00×10^{16}			
	InGaAs	Ec-0.9	2.67×10^{-11}	4.50×10^{14}	11.45	2.05	13.39
	InGaP	Ec-0.36	1.00×10^{-10}	8.00×10^{18}			
	InGaP	Ec-0.72	1.07×10^{-10}	9.00×10^{18}			
3.00E + 15	InGaP	Ev + 0.5	3.85×10^{-10}	2.00×10^{17}			
	InGaP	Ev + 0.76	6.17×10^{-10}	1.00×10^{17}			

extracted from the curve. The extracted values are listed in [Table 8](#).

From the results it is clear that deep level traps in conduction band like $Ec = -0.72$ and valance band = $Ev = +0.76$ are most significant, they create more recombination centers [\[26\]](#). Also higher energy radiation creates more traps. The increased trap concentration reduces the lifetime of the charge carriers and affects the electrical performance of the solar cell.

The variation in the trap concentration with fluence and the simulated carrier lifetime vs trap concentration is shown in [Fig. 12](#) for both top and middle cell. From the above figures it is clear that the trap concentration increases with the increase in the fluence [\[11,18\]](#). The carrier lifetime decreases with increase in trap concentration as per equation [\(3\)](#) and is due to traps acts as recommendation centers. Also, carrier lifetime decreases drastically with increase in fluence.

From different DLTS studies [\[8,18,27\]](#), it is found that at $Ec-0.36$, $Ec-0.72$ and $Ev + 0.5$ and $Ev + 0.76$ are the main non-radiative recombination centers for InGaP, whereas for GaAs is at $Ec-0.9$. In this simulation study, traps were introduced in both top GaInP and middle GaAs sub cells with the capture cross section as specified in [Table 4, 5](#). The trap concentrations were varied from 7×10^{17} to $9 \times 10^{18} cm^{-3}$ in top cell ($Ec-0.72$) and it varied from 2.5×10^{12} to $4.5 \times 10^{14} cm^{-3}$ in middle cell ($Ec-0.9$) for 10 MeV energy, similarly it is varied from 7×10^{17} to $3.2 \times 10^{18} cm^{-3}$ in top cell ($Ec-0.72$) and it varied from 2.3×10^{12} to $3 \times 10^{13} cm^{-3}$ in middle cell ($Ec-0.9$). Trap concentration increases with increased influence and energy this is because higher energy particles introduce more traps. The increased traps reduces the minority carrier life time and is shown in [Fig. 12](#).

The electrical parameters like short circuit current density Jsc, open circuit voltage Voc and conversion efficiencies were plotted as a function of trap concentration and is shown in [Fig. 13 a, b and c](#) for triple junction solar cell for both 1 MeV and 10 MeV electron radiation. The current density, open circuit voltage, and efficiency decrease for both 10 MeV and 1 MeV energy for all the fluences. The decrease observed is higher for higher energy, i.e. 10 MeV.

From the results it is clear that the electrical parameters degrade with increased trap concentration and energy. Both current and voltage decrease with traps and results in significant decrease in the efficiency, this can be attributed to radiation induced traps which acts as acceptor

Table 10

The details of trap level, lifetime trap concentration and JV parameters for 1 MeV electron radiation at both top and middle cell.

Electron radiation fluence e/cm ²	Material Type	Trap level	Lifetime in sec	Trap Concentration N _t (Cm ⁻³)	J _{sc} (mA/cm ²)	V _{oc} (V)	η (%)
BOL					17.875	2.61	28.95
1.00E + 14	InGaAs	Ec-0.9	5.23×10^{-9}	2.30×10^{12}			
	InGaP	Ec-0.36	1.34×10^{-9}	6.00×10^{17}			
	InGaP	Ec-0.72	1.37×10^{-9}	7.00×10^{17}			
	InGaP	Ev + 0.5	2.57×10^{-9}	3.00×10^{16}			
	InGaP	Ev + 0.76	2.47×10^{-9}	2.00×10^{16}			
5.00E + 14	InGaAs	Ec-0.9	1.85×10^{-9}	6.50×10^{12}	16.8	2.41	24.38
	InGaP	Ec-0.36	1.14×10^{-9}	8.0×10^{17}			
	InGaP	Ec-0.72	1.07×10^{-9}	9.00×10^{17}			
	InGaP	Ev + 0.5	1.10×10^{-9}	7.00×10^{16}			
	InGaP	Ev + 0.76	1.12×10^{-9}	5.50×10^{16}			
1.00E + 15	InGaAs	Ec-0.9	8.59×10^{-10}	1.40×10^{13}	16.35	2.37	21.94
	InGaP	Ec-0.36	5.34×10^{-10}	1.50×10^{18}			
	InGaP	Ec-0.72	4.81×10^{-10}	2.00×10^{18}			
	InGaP	Ev + 0.5	1.04×10^{-9}	7.40×10^{16}			
	InGaP	Ev + 0.76	9.94×10^{-10}	6.20×10^{16}			
3.00E + 15	InGaAs	Ec-0.9	4.01×10^{-10}	3.00×10^{13}	15.16	2.35	21.06
	InGaP	Ec-0.36	2.67×10^{-10}	3.00×10^{18}			
	InGaP	Ec-0.72	3.00×10^{-10}	3.20×10^{18}			
	InGaP	Ev + 0.5	9.63×10^{-10}	8.00×10^{16}			
	InGaP	Ev + 0.76	9.48×10^{-10}	6.50×10^{16}			

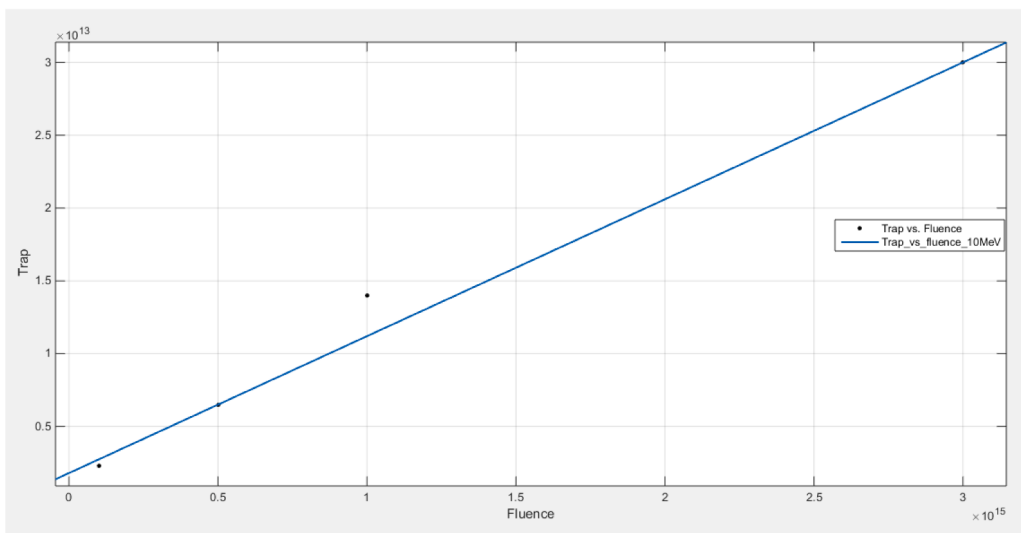


Fig. 11. Curve fitting for trap concentration and fluence(10 MeV).

and donor like energy states in the energy gap of the materials and reduces the band gap results in reduced voltage. The traps decrease the carrier life time. The lower carrier lifetime increases the recombination of charge carriers results in lower current generation and affects the electrical performance of the solar cell permanently.

5. Conclusion and further work

An extensive study of the effect of electron radiation on the triple-junction solar cell has been carried out in this paper using finite element analysis modeling. There is an increased emphasis on modeling the solar cell with more traps for different levels of energy and fluence in order to simulate radiation damage in the solar cells in space application. The current density -voltage characteristics are not only generated but also compared with the experimental JV data for the 1AM0 spectrum to further the validity of the modeling results. Using modeling, the effect of trap levels, type of traps, and trap concentration on cell parameters J_{sc}, V_{oc}, and efficiency η is studied for electron radiation of different

energy and fluences. Probable traps, carrier lifetime, and trap concentrations are extracted for different electron radiation energies and fluencies. The trap levels and trap concentration values of different energies and fluences illustrate the performance degradation of solar cell due to radiation induced defects. This study helps in the extraction of solar cell semiconductor properties, material selection, mole fraction and layer thickness optimization through simulations. These properties are useful in solar cell manufacturing process and the results can be invaluable as it can save significant R&D time and cost. Furthermore, these results obtained in this study can be used to develop a radiation model and predict the solar cell performance over a period of time of operation in space.

Declaration of Competing Interest

The authors declare that they have no known competing financial interests or personal relationships that could have appeared to influence the work reported in this paper.

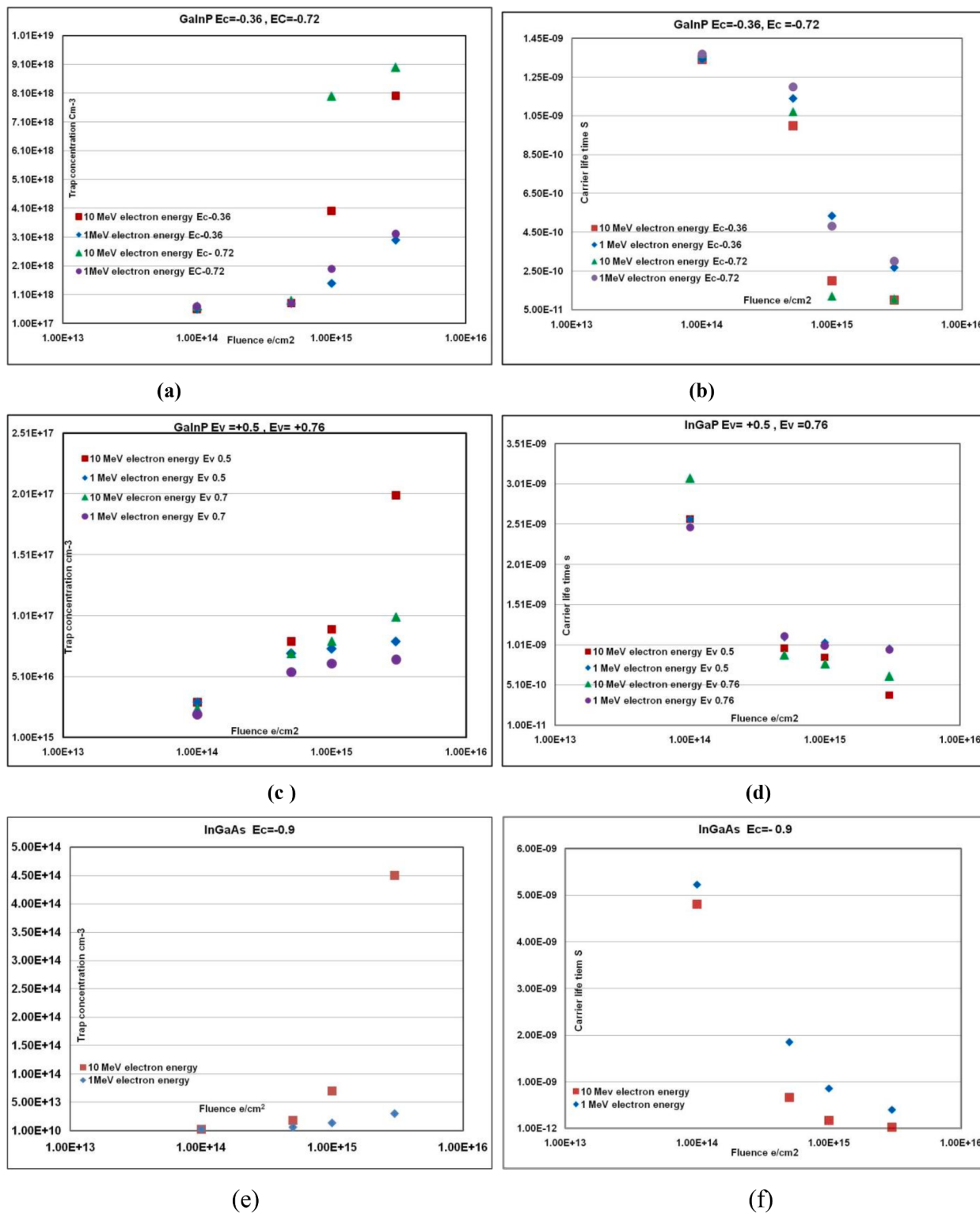


Fig. 12. Plots of Simulated output (a, c) trap concentration vs fluence, (b, d) Carrier lifetime vs trap concentration for InGaP top cell, (e) variation in the trap concentration vs fluence, (f) Carrier lifetime vs trap concentration for InGaAs middle cell (the data is taken from Table 4).

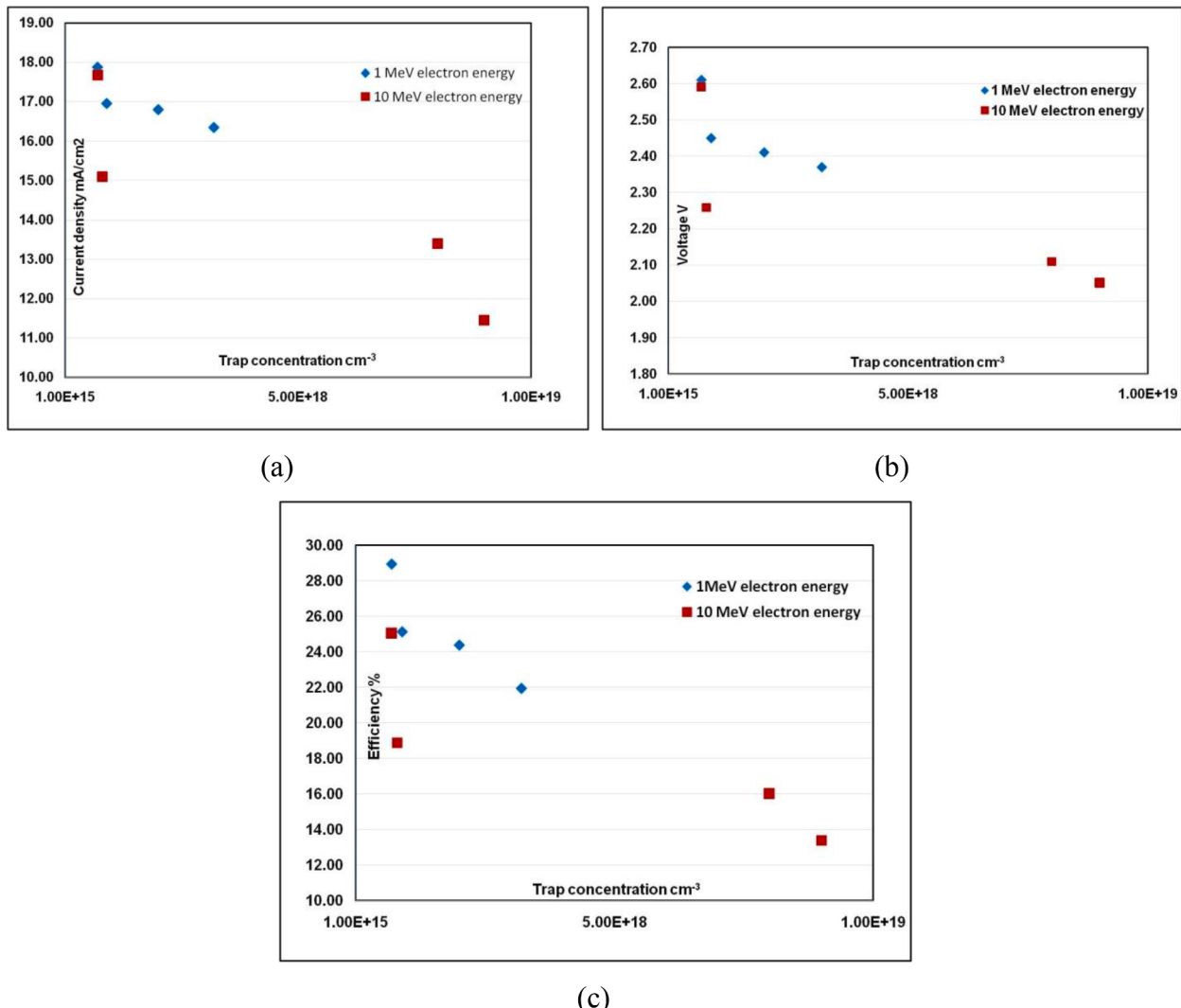


Fig. 13. Simulated output of GaInP/GaAs/Ge Triple junction solar cell (a) current density J_{sc} vs Trap concentration (b) Open circuit Voltage(V_{oc}) vs Trap concentration and (c) Efficiency vs Trap concentration for different electron 1 MeV and 10 MeV energies (table 9 and 10).

Data availability

Data will be made available on request.

Acknowledgement

This work was supported by the U.R. Rao satellite center (URSC). The radiation tests are carried out at Bhabha Atomic Research center (BARC), Electron Beam Center, Mumbai, Modeling is carried out by using Crosslight simulation software and Characterization is done at Solar panel division, URSC. Co-Author Mr. Ankush Saini is presently at IIT, Roorkee, India pursuing his research.

References

- [1] Antonio Luque, Steven Hegedus "Handbook of Photovoltaic Science and Engineering", Wiley, ISBN 0-471-49196-9, (2003).
- [2] Jongwon Lee, Christians B. Honsberg "Limiting Efficiencies of Integrating Single Junction with Intermediate Band Solar Cells for Multiphysics Effects" IEEE 40th Photovoltaic Specialist Conference, PVSC 2014, pp.1068-1072.
- [3] Indranil Bhattachary, "Design and Modeling of Very High-Efficiency Multijunction Solar Cells", Ph.D. Thesis, Florida State University Libraries.
- [4] M. Yamaguchi, III-V compound multi-junction solar cells: present and future, *Solar Energy Mater. Solar Cells* 75 (2003) 261–269.
- [5] R.I. Rabady, H. Manasreh, Thicknesses optimization of two- and three-junction photovoltaic cells with matched currents and matched lattice constants, *Solar Energy* (2017) 20–27.
- [6] B.E. Anspaugh, "GaAs Solar Cell Radiation Handbook", Jet Propulsion Laboratory, California Institute of Technology, 1996.
- [7] Daniel Derkacs, Dan Aiken, Zachary Bittner, Samantha Cruz, Alexander Haas, John Hart, Clay McPheeters, ChrisKerestes, Nate Miller, Pravin Patel, Michael Riley, Paul Sharps, Alex Stavrides, Claudia Struemel, and Steven Whipple "Development of IMM- α and Z4J Radiation Hard III-V Solar Cells" 45th IEEE PVSC 2018, DOI: 10.1109/PVSC.2018.8547857, pp.3757-3761.
- [8] Sherif Michael "A Novel Technique for modelling radiation effects in solar cells utilizing SILVACO virtual wafer fabrication software", RADECS proceedings, 2005, pp. LN9-1 to LN9-6.
- [9] Aaron L Crespin and Sherif Michael "Modelling the Effects of Electron Radiation in Solar Cells" 22nd AIAA International Communications Satellite Systems Conference and exhibit 2004. AIAA 2004-3269, pp. 1-5.
- [10] Z.Q. Li, Y.G. Xiao, Z.M. Simon Li. Modeling of multi-junction solar cells by Crosslight APSYS, Proceedings of SPIE - The International Society for Optical Engineering 6339 2006, pp. 633909-1 to 633909-8.
- [11] S. Kotamraju, M. Sukeerthi, S.E. Putthanveettil, M. Sankaran, Study the degradation in InGaP/InGaAs/Ge Multijunction Solar cell characteristics due to irradiation-induced deep level traps using finite element analysis, *Solar Energy* 178 (2019) 215–221.
- [12] P.R. Sharps, D.J. Aiken, M.A. Stan, C.H. Thang, N. Fatemi, Proton electron radiation data and analysis of GaInP₂/GaAs/Ge solar cells, *Prog. Photovoltaics: Res. Appl.* (2002) 383–390.
- [13] A. Khan, M. Yamaguchi, J.C. Bourgoin, N. de Angelis, T. Takamoto, Room-temperature minority-carrier injection-enhanced recovery of radiation-induced defects in p-InGaP and solar cells, *Appl. Phys. Lett.* 76 (2000) 2559–2561.

- [14] J.C. Bourgoin, M. Zazoui, Irradiation-induced degradation in solar cell: characterization of recombination centers, *Semiconductor Sci. Technol.* 17 (2002) 453–460.
- [15] S. Asif, Y. Li, Solar cell modeling and parameter optimization using simulated annealing, *J. Propul. Power* 24 (5) (2008) 1018–1022.
- [16] L. Gelczuk, M.D. Abrowska-Szata, B.S. Ciana, D. Pucicki, D. Radziewicz, K. Kopalko, M. Tlaczala, Characterization of deep-level defects in GaNAs/GaAs heterostructures grown by APMOVPE, *Mater. Sci.-Poland* 34 (4) (2016) 726–734.
- [17] H. Mazouz, P.-O. Logerais, A. Belghachi, O. Riou, F. Delaleux, Effect of electron irradiation fluence on the output parameters of GaAs solar cell, *Int. J. Hydrogen Energy* 40 (39) (2015) 13857–13865.
- [18] Aurangzeb Khan, Masafumi Yamaguchi “Minority carrier injection-enhanced recovery of radiation-induced defects in P-InGaP and solar cells”, 28th IEEE Photovoltaic Specialists Conference2000, pp. 1106-1109.
- [19] A. Khan, M. Yamaguchi, N. Dharmaso, J. Bourgoin, T. Takamoto, Deep Level spectroscopy analysis of 10MeV proton and 1MeV electron irradiation induced defects in p-InGaP and InGaP based solar cells, *J. Appl. Phys.* 41 (2002) 1241–1246.
- [20] H. Mazouz, A. Belghachi, F. Hadjaj. Solar cell degradation by electron irradiation effect of irradiation fluence” World Academy of science engineering and technology,
- [21] International journal of Physical nuclear science and engineering 7(12) 2013 1718–1720.
- [22] D.V. Lang, L.C. Kimerling, S.Y. Leung, Recombination enhanced annealing of the E1 and E2defect levels in 1MeV electron-irradiated nGaAs, *J. Appl. Phys.* 47 (3587) (1976) 3587–3591.
- [23] D.V. Lang, R.A. Logan, L.C. Kimerling, Identification of the defect state associated with a gallium vacancy in GaAs and Al_xGa_{1-x}As, *Phys. Rev. B* 15 (10) (1977) 4874.
- [24] C. Baur, A.W. Bett, “Modeling of the degradation of iii-v triple-junction cells due to particle irradiation on the basis of component cells” IEEE2010, pp.1100-1105.
- [25] Nethaji Dharmarasu, Masafumi Yamaguchi, Aurangzeb Khan”High-radiation-resistant InGaP, InGaAsP, and InGaAs solar cells for multijunction solar cells”, *Appl. Phys. Lett.* 79, 2399 (2001) 10.1063/1.1409270.
- [26] B. Danilchenko, A. Budnyk, L. Shpinar, D. Poplavskyy, S.E. Zelensky, K.W. J. Barnham, N.J. Ekins-Daukes, 1 MeV electron irradiation influence on GaAs solar cell performance, *Solar Energy Mater. Solar Cells* 92 (2008) 1336–1340.
- [27] Y. Yana, M. Fangc, X. Tang, F. Chen, H. Huang, X. Suna, L. Jia, Effect of 150 keV proton irradiation on the performance of GaAs solar cells, *Nucl. Inst. Methods Phys. Res. B* 451 (2019) 49–54.